# Breakup and coalescence of free surface flows

The picture of a dolphin, jumping out of the water in the New England aquarium in Boston (Fig.1), gives a very good idea of the challenges involved in the description of free-surface flows. In a complex series of events, which is still not well understood, water swept up by the dolphin breaks up into thousands of small drops. A more detailed idea of what happens close to the point of breakup is given in Fig.2, which shows a drop of water falling from a faucet. Once an elongated neck has formed, surface energy is minimized by locally reducing its radius, and a drop separates at a point. Once the neck is broken, it rapidly snaps back, forming a capillary waves on its surface. In the last picture on the right, the neck has been severed on the other end as well. Thus in a single dripping event, two drops have actually formed, and the smaller "satellite" drop will subsequently break up to form even smaller drops. This gives a good idea of the complexity of just a single breakup event, driven by surface tension.

The complementary event of drop coalescence is illustrated by Fig.3, which shows two drops which have been made to touch at a point. Surface tension drives a motion that makes the drop coalesce, since the combined drop has a lower surface energy. The intitial motion is so rapid that it is hardly resolved by the camera, and it results in quite a complicated sequence of capillary waves, drop oscillations, etc.

Clearly changes in topology brought about by breakup or coalescence are the most dramatic events in the evolution of a free surface, characterized by a very rapid and complex motion of the surface (cf. Figs.2 and 3). In fact, it is not a priori clear whether continuum equations are able to describe topology changes, since somewhere in between flow features develop which are of molecular size. So apart from predicting the actual motion near the singular point, the aim of the theory is to explain how one topology can be transformed in the other in a unique way. The spatial and temporal resolution of any numerical simulation is limited, so a thorough understanding of the singularity is needed. Once the rapid motion near the singularity can be described theoretically, the numerical evolution can be matched onto it. In addition, the theoretical description of singularities will explain some universal flow features, attributable to breakup or coalescence of drops.

## Non-linear dynamics of drop formation

To obtain insight into the non-linear dynamics close to breakup one has to solve a notoriously difficult problem: the Navier-Stokes equation within a domain that is changing in time. The motion of the interface is dictated by the fluid motion itself, as the interface is convected passively by the fluid motion at the interface. The motion of the interface has to be computed with great accuracy, because the fluid motion is driven by surface tension, resulting in a Laplace pressure proportional to the mean curvature of the interface. Since the driving is

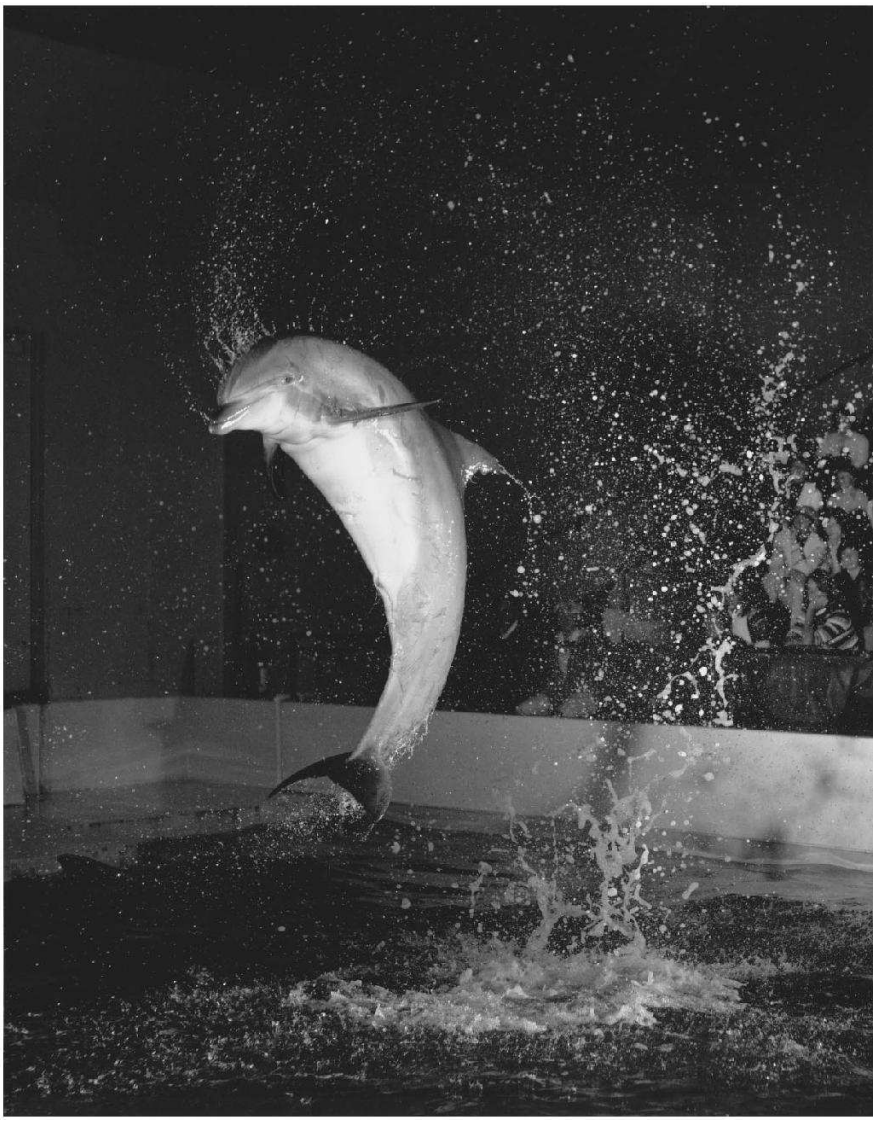

Figure 1: Dolphin in the New England aquarium in Boston; photograph by Harald Edgerton.

proportional to pressure *gradients*, acceleration of a fluid element is effectively determined by *third derivatives* of the surface shape. The numerical difficulties inherent in this coupling of fluid motion and its driving force are discussed thoroughly by Scardovelli and Zaleski (1999), giving an overview of available numerical methods.

To obtain greater insight into drop breakup, it is necessary to reduce the non-linear dynamics associated with it to its essentials. The idea is that near the point where the neck radius goes to zero, the fluid motion is directed primarily in a direction parallel to the axis. This allows to reduce the problem to an equation for the average velocity in the axial direction alone. Alternatively, and more or less equivalently, the velocity field can be expanded in the radial co-ordinate. If a typical radial length scale is smaller than the corresponding axial one, usually signaled by the interface slope being less than one, the leading order coefficient for the velocity suffices, as discussed in detail by Eggers (1997).

The result is a system of equations for the local radius $h(z,t)$ of the fluid neck, and the average velocity $v(z,t)$ in the radial direction. All other terms are of higher order in $h$ or the radial variable $r$. For a liquid with kinematic viscosity $\nu$, density $\rho$, and surface tension $\gamma$ (neglecting the effect of the outer gas), the result of the calculation is:

$$\partial_t h^2 + \partial_z (v h^2) = 0, \tag{1}$$

$$\underbrace{\partial_t v + v \partial_z v}_{\text{inertia}} = \underbrace{-\frac{\gamma}{\rho} \partial_z \left( \frac{1}{R_1} + \frac{1}{R_2} \right)}_{\text{surface tension}} + \underbrace{3\nu \frac{\partial_z (\partial_z v h^2)}{h^2}}_{\text{viscosity}} . \tag{2}$$

The simplification achieved by (1),(2) is enormous. Firstly, the dimension of the problem been reduced by one (the radial variable has been eliminated). Secondly, the moving boundary has been described explicitely by $h(z,t)$. Equation (1) expresses the conservation of mass: it is written as a conservation equation for the volume $h^2 dz$ of a slice of fluid. Equation (2) is a balance of forces acting on a fluid element, and thus very similar in structure to the original Navier-Stokes equation (Landau and Lifshitz (1984)). The l.h.s. of (2) corresponds to inertial forces, driven by surface tension and viscous forces on the right. As to be expected from Laplace's formula, surface tension forces are proportional to the mean curvature, which for a body of rotation is

$$\frac{1}{R_1} + \frac{1}{R_2} = \frac{1}{h\sqrt{1+(\partial_z h)^2}} - \frac{\partial_{zz} h}{\sqrt{1+(\partial_z h)^2}^3}. \tag{3}$$

Strictly speaking, the radial expansion implied by (1),(2) would have required us to replace the mean curvature by the leading-order expression $1/h(z,t)$ alone. This is indeed sufficient to describe the neighborhood of the pinch point, but the applicability of the equations is greatly enhanced by including the full curvature, because the equations then include a

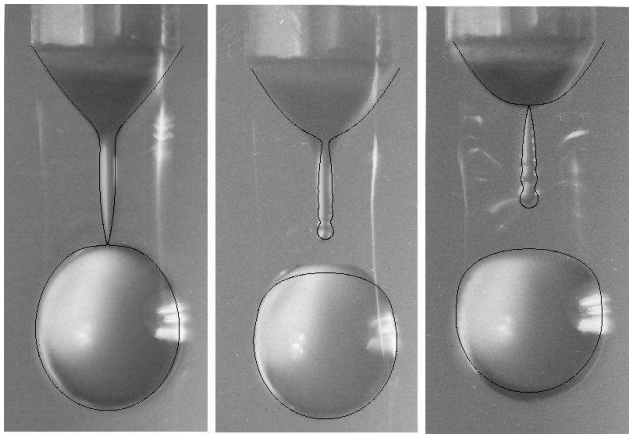

Figure 2: A sequence of photographs showing a drop of water falling from a pipette $D = 5.2mm$ in diameter (photograph by H. Peregrine, see Eggers (1997)). The superimposed black lines are the result of a simulation of the one-dimensional equations (1),(2).

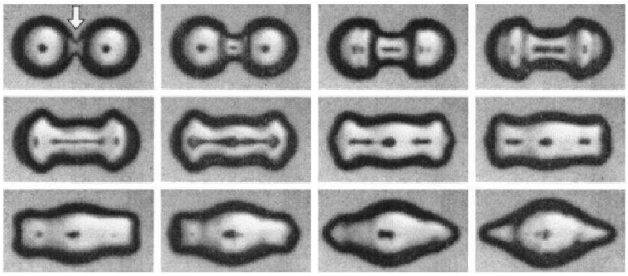

Figure 3: A sequence of images ($\Delta t = 1ms$) of two mercury drops brought into contact at the point indicated by an arrow (Menchaca-Rocha et al. (2001)).

spherical drop among its equilibrium solutions.

The remarkable power of the system (1),(2) in describing a real break-up event is illustrated by Fig.2. The sequence of experimental pictures shows a drop of water falling from a pipette 5.2 mm in diameter. The drop is shown at the moment of the first bifurcation (first picture), after which the fluid neck recoils from the drop (second picture). Shortly afterward the neck pinches on its other end (third picture), thereby forming a "satellite drop". Such satellite drops are seen to be a direct consequence of the long neck that is forming at pinch-off, which in turn reflects the profile being extremely asymmetric around the pinch-point: on one side, the profile asymptotes to the drop, on the other side it is very flat and forms a slender neck.

It is evident from Fig.2 that the one-dimensional approximation works extremely well in describing breakup, and the formation of satellite drops. This includes regions near the drop, where the profile is actually quite steep, so the expansion underlying (1),(2) is formally not valid. A careful assessment of the quality of one-dimensional approximations, achieved through comparison with accurate numerical simulations of the full Navier-Stokes equation,

is given in Ambravaneswaran et al. (2002). As discussed in the introduction, it is not clear how to pass from the first panel in Fig.2 to the second on the basis of (1),(2), but rather some "surgery" was necessary. Namely, when the minimum neck radius was just $10^{-4}$ times the original radius, it was cut and spherical caps were placed on either side. Below we will justify this procedure on the basis of a more detailed understanding of the dynamics at the pinch point.

## Similarity solutions

We now turn to the immediate neighborhood of the pinch point, where separation occurs. Since the evolution takes place on length and time scales much smaller than any externally applied scales such as the diameter $D$ of the capillary in Fig.2, the motion should be properly measured in some *intrinsic* units of the fluid. The only such units of length and time that can be formed from the fluid parameters are

$$\ell_\nu = \frac{\nu^2\rho}{\gamma} \text{ and } t_\nu = \frac{\nu^3\rho^2}{\gamma^2}. \tag{4}$$

As expected intuitively, length and time scales increase with viscosity, which can vary greatly between different fluids. For water, the viscous length scale $\ell_\nu$ is just 10 nanometers, far below anything visible on the scale of the photographs in Figs.2 and 3. For glycerol, on the other hand, $\ell_\nu$ is in the order of centimeters, and the asymptotics described below is easily observable.

Since our description is local, it is clear that we have to represent the motion in a local co-ordinate system. The only reasonable choice for its origin is the point $z_0$ and time $t_0$ where the singularity occurs. Making space and time dimensionless using $\ell_\nu$ and $t_\nu$, we introduce

$$z' = (z - z_0)/\ell_\nu \text{ and } t' = (t_0 - t)/t_\nu. \tag{5}$$

Now representing the spatial profile as well as the velocity field in these co-ordinates,

$$\begin{aligned} h(z,t) &= \ell_\nu H(z',t') \\ v(z,t) &= \frac{\ell_\nu}{t_\nu} V(z',t') \end{aligned} \tag{6}$$

we expect the new functions $H$ and $V$ to represent properties of the singularity alone. In particular, we hope that they are *universal*, independent of both the initial conditions and the material parameters of the fluid.

Since no external scales are thus expected to come into play in the description of $H(z',t')$ and $V(z',t')$, these profiles should be invariant under a change of scale. This means both

the height and the velocity profile should be *self-similar*:

$$H(z',t') = t'\phi\left(\frac{z'}{t'^{1/2}}\right)$$
$$V(z',t') = t'^{-1/2}\psi\left(\frac{z'}{t'^{1/2}}\right). \tag{7}$$

The meaning of (7) is that the shape of the profiles does not change as a function of time, only the radial, axial, and temporal scales are adjusted as $t'$ goes to zero. The exponents implicit in (7) were computed from the requirement that all terms in the equations balance, i.e. that inertial, surface tension, and viscous forces are of the same order close to the singularity.

In particular, two things are noteworthy about the exponents: First, the neck radius shrinks linearly with $t'$ as the singularity is approached, while the corresponding axial scale only shrinks like $t'^{1/2}$. This implies that the profile is asymptotically slender, and the assumptions underlying the derivation of (1),(2) were justified. Second, the exponent of the velocity is negative, so the motion is increasingly fast close to the singularity. This is not unexpected, since ever stronger surface tension forces are driving increasingly small fluid necks. Once the neck reaches microscopic size, of course, the description in terms of a velocity field becomes meaningless, so there is no danger of truly infinite velocities looming here.

Finally, once the self-similar form (7) is re-introduced into the equations of motion (1),(2), one obtains a set of *ordinary differential equations* for the similarity profiles $\phi(\xi)$ and $\psi(\xi)$ alone. A more thorough analysis of the structure of the equations reveals (Eggers (1997)) that there is only one universal solution of them, once proper boundary conditions are imposed at $\xi = \pm\infty$. These are derived from the condition that matching must be possible to the macroscopic profiles farther away, which evolve on much longer timescales than the self-similar solution itself. A remarkable consequence of this universality is that the minimum neck radius, at a given time away from the point of breakup, is a quantity that is *independent* of the initial radius (Eggers (1997)):

$$h_{min} = 0.03\frac{\gamma}{\nu\rho}(t_0 - t). \tag{8}$$

To look at a comparison between theory and experiment in more detail, Fig.4 shows three successive images of a jet of glycerol pinching off to form a drop (a small section of which is seen on the right). Once the temporal distance from the singularity is known (from experiment), the profile can be predicted without adjustable parameters (dark continuous lines). The only difference between the three sets of lines is that the axes have been rescaled by the factor implied by (7).

The universality of the solution described by (7) of course implies that it holds equally well

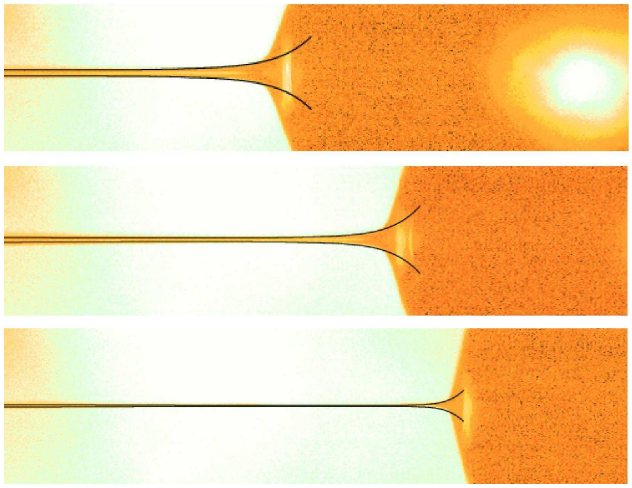

Figure 4: A sequence of interface profiles of a jet of glycerol close to the point of breakup (the center of the drop being formed is seen as a bright spot in the top picture). The experimental images correspond to $t_0 - t = 350\mu s, 298\mu s$, and $46\mu s$ (from top to bottom). Corresponding analytical solutions based on (7) are superimposed. (Experiment by T. Kowalewski, see Eggers (1997))

for the pinching of the drop of water shown in Fig.2, as it does for the glycerol jet of Fig.4. The reason this common feature is not immediately apparent is that $\ell_\nu$ is extremely small for water, so one would have to observe the neighborhood of the point of breakup in Fig.2 under extreme magnification. This means that only on a very small scale will all three forces contributing to (2) come into play. For the parts of the evolution where the minimum radius $h_{min}$ is much larger than $\ell_\nu$, one can neglect viscosity, so that Fig.2 is effectively described by inviscid dynamics.

Thus to understand the appearance of drop pinch-off on a given scale $D$ (such as the nozzle diameter), one has to take into account the phenomenon of crossover: if initially $D \gg \ell_\nu$, the dynamics is characterized by a balance of inertial and surface tension forces. As $h_{min}$ reaches $\ell_\nu$, the dynamics changes toward an inertial-surface tension-viscous balance. If on the other hand $D \ll \ell_\nu$ initially, inertia cannot play a significant role: the dynamics is dominated by viscosity and surface tension. In the course of this evolution, however, inertia becomes increasingly important and finally catches up with the other two. As a result, the same universal solution as before is finally observed.

To each of the new balances described above corresponds a new similarity solution, distinct from (7) (Eggers (1997)). For example, the inertia-surface tension balance leads to a minimum drop radius that behaves like

$$h_{min} = 0.7 \left(\frac{\gamma}{\rho}\right)^{2/3} (t_0 - t)^{2/3}, \tag{9}$$

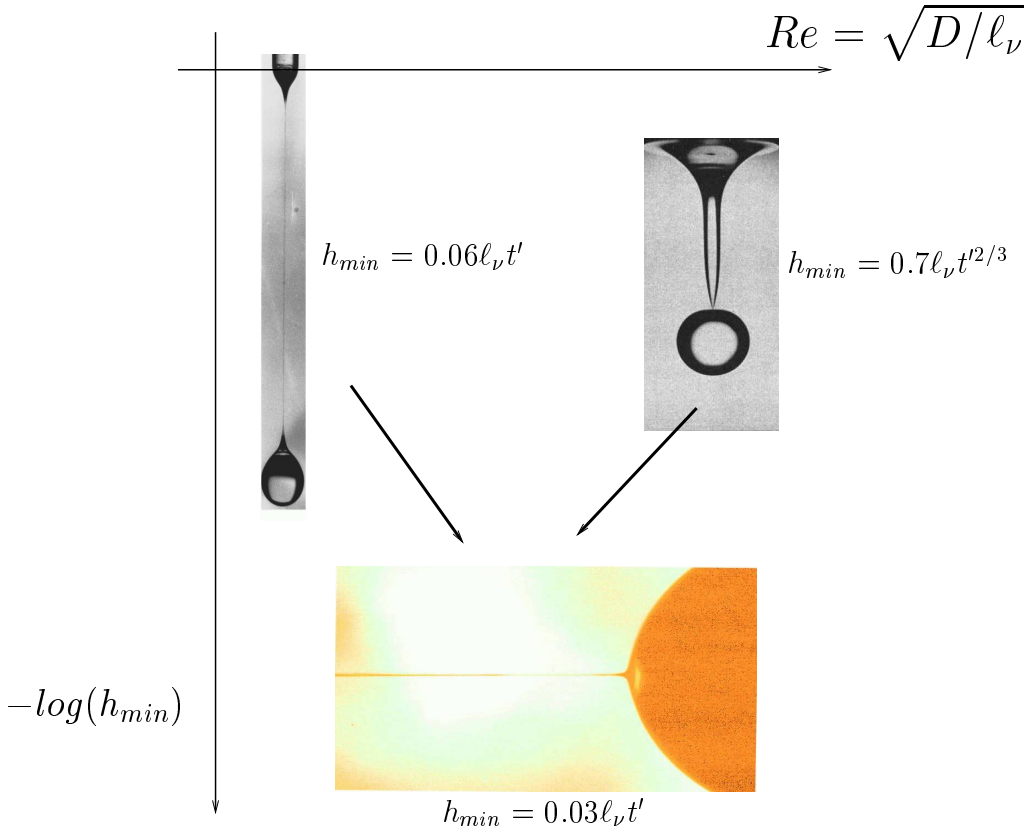


Figure 5: A graphical representation of some of the scaling regimes that can be observed in droplet pinching, depending on the viscosity of the liquid. For high viscosity ($Re$ small) threads form as a drop falls from a pipette of diameter $D$. In the opposite case of low viscosity ($Re$ large) the pinching neck is conical. As the neck radius goes to zero, however, one always ends up with the same universal scaling regime. (Photographs by X.D. Shi and S. Nagel, see Eggers (1997))

while the viscous-surface tension balance corresponds to

$$h_{min} = 0.06\frac{\gamma}{\nu\rho}(t_0 - t). \tag{10}$$

The spatial structure of the corresponding similarity solutions largely explains the macroscopic appearance of high and low viscosity fluids, respectively. The axial and radial scales of the inviscid solution (9) both behave like $(t_0 - t)^{2/3}$, thus leading to a neck that is cone-shaped, consistent with Fig.2. For its computation, the lubrication equations (1),(2) are inadequate, rather, the full equations for inviscid, irrotational flow have to be solved. The reason is that the interface profile *turns over*, so that the tip of the cone-shaped neck is actually inside the drop. These predictions of similarity theory have been confirmed by both experiment and full numerical simulations of the Navier-Stokes equations by Chen et al. (2002).

Very viscous fluids, on the other hand, tend to form very elongated threads. This is reflected by the fact that the typical axial scale of the viscous solution (10) behaves like $(t_0 - t)^{0.175} \gg (t_0 - t)$. Interestingly, the exponent $\beta = 0.175\ldots$ is an irrational number coming from the solution of a transcendental equation (Eggers (1997)). This is an example of self-similarity of the second kind, in the classification of Barenblatt (1996). The striking difference in the behavior of high and low viscosity fluids is represented schematically in Fig.5.

It would be beyond the scope of this brief overview to mention all the recent developments in the study of drop pinch-off, some of which are discussed in Lin (2003). To name some examples, the presence of an outer fluid significantly alters pinching, leading to new types of similarity solutions, with important applications for the physics of mixing. For extremely small jets of the size of nanometers, thermal fluctuations have to be taken into account, which significantly alter the dynamics. This has been found using *molecular dynamics* simulations of a jet 6 nanometers in diameter. However, even on much larger scales small perturbations to the observed similarity solutions can be important. In fact, the threads shown in Fig.4 are quite sensitive to perturbations, and a careful examination of the last panel shows (unfortunately obscured by the drawn lines) the growth of disturbances on the thread Eggers (1997).

In other words, the question of what resolution (experimental or numerical) is necessary near the point of breakup depends very much on what one is interested in: a lot of detail may be buried within a pinching event, which may or may not be important for a given question.

If one is trying to describe topological transitions numerically, one will always have to renounce the description of the dynamics below some cutoff length. It is therefore important to understand the mechanisms which guarantee the uniqueness of the continuation across the singularity. The key is again the universality of similarity solutions we already found in the approach to the singularity. A new set of similarity solutions can be found after breakup

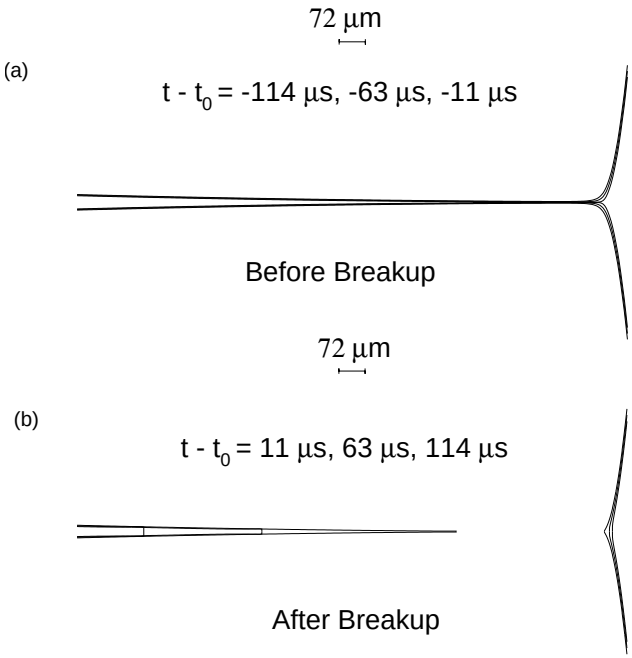


Figure 6: The breakup of a mixture of glycerol in four parts of ethanol, as calculated from similarity solutions before and after breakup. Part (a) shows three profiles before breakup, in time distances of 46 $\mu$s, corresponding to $|t'| = 1, 0.55$, and 0.1. In part (b) the same is shown after breakup.

- one exists on either side of the pinch point. This is illustrated in Fig.6, which shows some typical predictions of the similarity theory. On one side one sees the rapid retraction of a very thin needle, on the other a small protrusion is left initially on the drop, which quickly heals off to form a smooth drop.

The difference to the similarity solution before breakup lies of course in the boundary condition at the retracting tip. A closer analysis reveals (Eggers (1997)) that the similarity solutions after breakup depends on the boundary conditions for both the height and the velocity as one moves away to infinity. The crucial condition that guarantees unique continuation is the fact that both profiles to the left and right of the point of breakup have to coincide with the solutions *before* breakup as one moves to infinity. Information between the solutions before and after breakup is thus passed on solely on the basis of the far-field behavior. Whatever microscopic physics determines the actual breakup event is irrelevant to the continuation.

## Coalescence

As we have seen above, the understanding of drop breakup is aided greatly by the universality of the observed solutions. One is able to almost completely disregard the free-surface motion away from the point of breakup. The main difficulty in finding a unifying picture for drop

coalescence lies in the fact that one cannot disregard the drop motion that leads to the meeting of the two drops, resulting in a number of problems.

Firstly, the motion produced by the purely geometrical overlap between two approaching drops is comparable or faster than the motion generated by surface tension. Hence the velocity of approach must come into play when describing the dynamics of coalescence. Secondly, the fluid caught between two approaching drops cannot be ignored, even if its viscosity is very small. The reason is that a very thin lubrication film between two drops will still produce an appreciable pressure, which deforms the drops prior to their meeting at a point. Thirdly, the mechanism that leads to the first small-scale union between the drops is not well understood. In particular, the presence of surfactants on the surface produces barriers that have to be overcome, which can significantly delay reconnection, as shown by Amarouchene et al. (2001).

We will therefore focus on the simplest case of a vanishing speed of approach, in which case the ensuing dynamics is determined by the fluid parameters and the radius $R$ of the drops alone. If the two drops do not have equal radius, the one with the smaller radius will play the dominant role and effectively replace $R$. Since the motion starts from rest, it will initially be slow, so the driving by surface tension is counteracted by viscosity alone. This behavior will persist until the radius $r_m$ of the liquid bridge connecting the two drops has reached $\ell_\nu$, after which it crosses over to one where only inertia matters and viscosity drops out of the problem. Finally, for $r_m \approx R$, the initially local motion in the bridge between the drops evolves to a global motion involving all of the fluid.

The central idea in investigating the dynamics of coalescence is of course that for $r_m \ll R$ the motion is self-similar, dominated by the local behavior close to the meniscus where the two drops meet. At the meniscus the curvature is extremely high, and thus leads to a driving that is confined to a ring-shaped region, whose radius $r_m$ is expanding. Turning first to the initial stage of viscous motion, the problem is thus one of a *line force* moving through an infinite medium. The force per unit length of the line is $2\gamma$, and one has to compute the speed that results from it. It is one of the characteristic features of Stokes flow that to obtain a finite answer, logarithmic corrections come into play, for which an upper and a lower cut-off is needed. The upper cut-off evidently is the radius of the drop itself, the width of the meniscus serves as the lower cutoff. The result of the calculation (Eggers et al. (1999)) is ($\eta = \nu\rho$ being the viscosity):

$$r_m(t) \sim -\frac{\gamma}{\eta}\frac{(\alpha-1)}{2\pi} t \ln \frac{\gamma}{R\eta} t, \tag{11}$$

where the width of the meniscus $\Delta$ is assumed to scale like $\Delta \propto r_m^\alpha$.

Interestingly, the value of $\alpha$ which determines the prefactor in (11) depends on the presence of an outer fluid between the drops. If no outer fluid is present, the correct value is $\alpha = 3$,

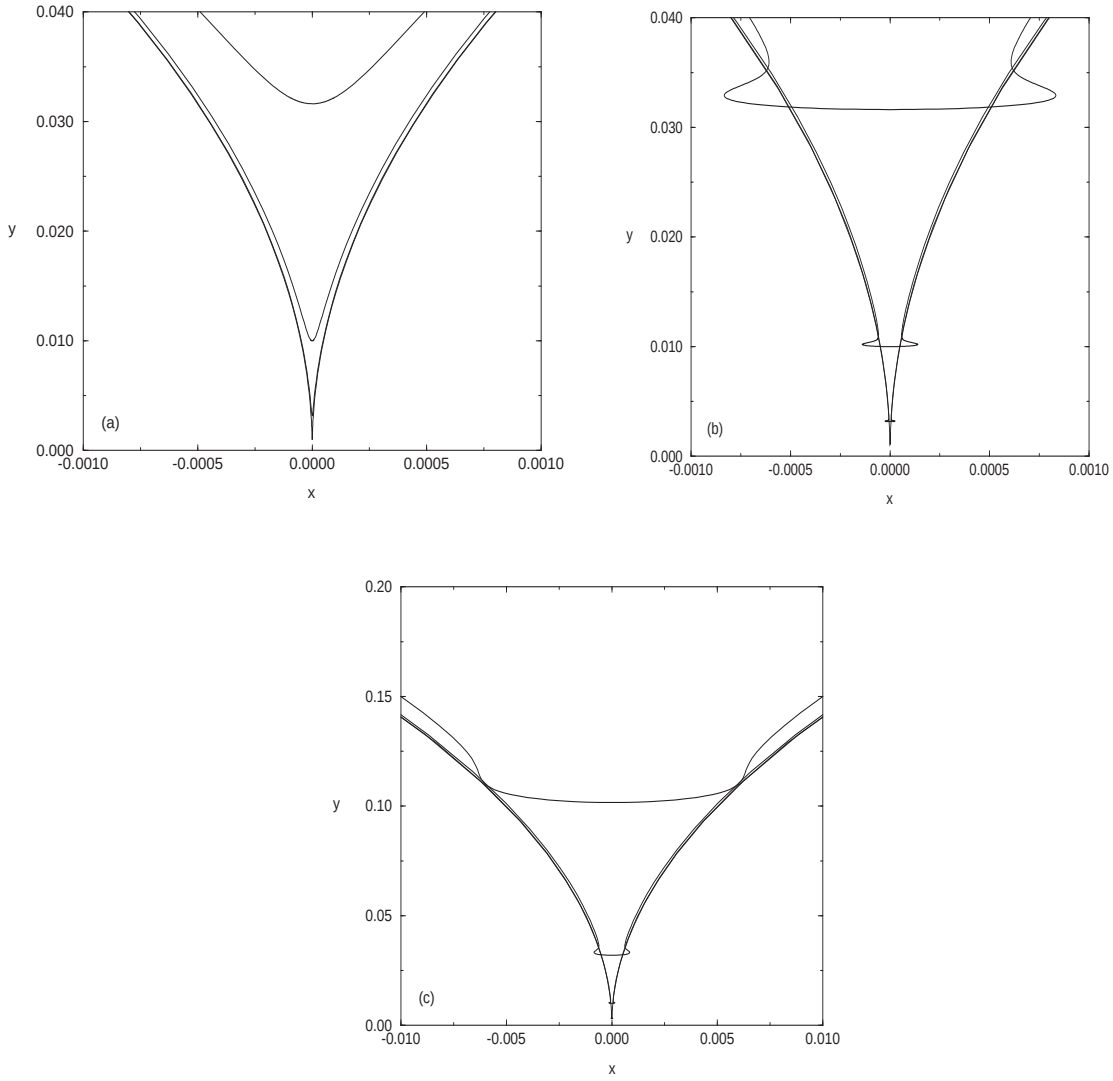


Figure 7: A closeup of the point of contact during coalescence of two identical drops for the two cases of no outer fluid, (a), and two fluids of equal viscosity, ((b) and (c)). Part (a) is Hopper's solution (no outer fluid) for $r_m/R = 10^{-3}, 10^{-2.5}, 10^{-2}$, and $10^{-1.5}$. Part (b) is a numerical simulation of the case where the inner and outer viscosities are the same, showing fluid that collects in a bubble at the meniscus. Note that the two axes are scaled differently, so the bubble is almost circular. For large values of $r_m$, as shown in (c), the fluid finally escapes from the bubble.

which can in fact be deduced from an *exact* solution (due to Hopper) to the two-dimensional analogue of the problem under study (Eggers et al. (1999)). A closeup of this extremely sharp meniscus is shown in panel (a) of Fig.7. Even a small amount of interstitial fluid, however, changes the situation considerably. Owing to the fact that the gap between the drops is exceedingly narrow, it is quite hard to push any fluid away from the advancing meniscus. Instead, the interstitial fluid is collected in a pouch at the meniscus (see Fig.7), and $\Delta$ is now much larger, so that one finds $\alpha = 3/2$ (Eggers et al. (1999)).

If the drop fluid is very viscous ($\ell_\nu > R$), this is all that can be said from the point of view of aymptotics. Among others, we have established that the motion is described by a well-defined asymptotic solution. Hence after a very short time, details of the microscopic mechanisms leading to coalescence have been "forgotten". In a numerical simulation, "surgery" done on a sufficiently small scale will meet a similar fate, and on soon ends up following the unique physical solution.

Finally, if $\ell_\nu \ll R$, there is a region where the motion is almost inviscid. From a balance of surface tension forces with inertial forces at the meniscus one deduces (Eggers et al. (1999)) that

$$r_m \propto \left(\frac{\gamma R}{\rho}\right)^{1/4} t^{1/2}. \tag{12}$$

This behavior has been confirmed by recent numerical simulations of Duchemin et al. (2003). However, there is an unexpected complication: as the meniscus retracts, capillary waves grow ahead of it, whose amplitude finally equals the width of the channel. Thus the two sides of the drops touch, and a toroidal void is enclosed. This process repeats itself, leaving behind a self-similar succession of voids.

In summary, one can often obtain analytical solutions to the equations of motion near a singularity, explaining some universal features of breakup and coalescence events. This is important for estimating errors introduced by a given numerical procedure used to describe topological transitions. Matching numerics to known analytical solutions can lead to considerable savings in numerical effort.

## Bibliography


R. Scardovelli and S. Zaleski, "Direct numerical simulation of free-surface and interfacial flow", Annu. Rev. Fluid Mech. **31**, 567-603 (1999).

J. Eggers, "Non-linear dynamic and breakup of free-surface flows", Rev. Mod. Phys. **69**, 865-929 (1997).

L. D. Landau and E. M. Lifshitz, *Fluid Mechanics* Pergamon, Oxford (1984).

A. Menchaca-Rocha et al., "Coalescence of liquid drops by surface tension", Phys. Rev. E **63**, 046309,1-5 (2001).

B. Ambravaneswaran, E.D. Wilkes, and O.A. Basaran, "Drop formation from a capillary tube: Comparison of one-dimensional and two-dimensional analyses and occurence of satellite drops. Phys. Fluids **14**, 2606-2621 (2002).

A.U. Chen, P. K.Notz, and O.A. Basaran, "Computational and Experimental Analysis of Pinch-Off and Scaling" Phys. Rev. Lett. **88**, 174501,1-4 (2002).

G.I. Barenblatt, *Scaling, Self-Similarity, and Intermedeate Asymptotics*, Cambridge (1996).

S.P. Lin, *Breakup of liquid sheets and jets*, Cambridge (2003).

Y. Amarouchene, G. Cristobal, H. Kellay, "Noncoalescing Drops", Phys. Rev. Lett. **87**, 206104, 1-4 (2002).

J. Eggers, J. R. Lister, and H. A. Stone, "Coalescence of Liquid Drops", J. Fluid Mech. **401**, 293-310 (1999)

L. Duchemin, J. Eggers, and C. Josserand, "Inviscid Coalescence of Drops", J. Fluid Mech. **487**, 167-178 (2003)

Jens Eggers
School of Mathematics, University of Bristol,
University Walk, Bristol BS8 1TW, UK
jens.eggers@bris.ac.uk